doi:10.3788/gzxb20164501.0106001

单入射波长及纤芯存在光致双折射的长周期光纤光栅的折射率传感分析

白育堃[1,2],张玥[1],马秀荣[1]

(1 天津理工大学 计算机与通信工程学院 通信器件与技术教育部工程研究中心,天津 300384)

(2 天津大学 精密仪器与光电子工程学院 激光与光电子研究所 光电信息科学技术教育部重点实验室,天津 300072)

摘 要:利用全矢量耦合模方程提出并分析了一种基于纤芯存在光致双折射的长周期光纤光栅的环境折射率传感测量方法.以波长为谐振波长的完全偏振光为入射波,通过分析不同环境折射率下输出光的偏振态在邦加球上与参考点间球面距离的变化测量环境折射率.分析表明,在环境折射率 1～1.30 范围内包层半径为 20.75 μm 的长周期光纤光栅传感器线性特性良好,灵敏度为 0.356/RIU,可应用于湿度和气体的折射率测量;该分析方法适用于其他类型的双折射长周期光纤光栅传感器的设计.

关键词:双折射;长周期光纤光栅;全矢量耦合模方程;斯托克斯参数;光纤光学传感

中图分类号:TP212 **文献标识码**:A **文章编号**:1004-4213(2016)01-0106001-5

Analysis of Refractive Index Sensing Based on the Core-Only Birefringent Long-period Fiber Grating with Single Wavelength

BAI Yu-kun, ZHANG Yue, MA Xiu-rong

(1 *Engineering Research Center of Communication Devices and Technology, Ministry of Education, School of Computer and Communication Engineering, Tianjin University of Technology, Tianjin* 300384, *China*)

(2 *Key Laboratory of Optoelectronic Information Science and Technology, Ministry of Education, Institute of Laser and Optoelectronics, College of Precision Instrument and Optoelectronics Engineering, Tianjin University, Tianjin* 300072, *China*)

Abstract: Using the full-vector coupled mode theory, a method for Surrounding Refractive Index (SRI) sensing with a single wavelength was proposed which is based on the core-only photoinduced birefringence of Long-Period Fiber Grating (LPFG). With a completely-polarized light near the resonant wavelength launched into the LPFG, the variation of the spherical distances between the output light polarization states for various SRIs and that for the reference SRI=1 on the Poincare sphere is investigated to identify the SRIs. The analysis indicates that the SRI sensor with a cladding radius of 20.75 μm shows a good linearity performance and high sensitivity of 0.356/RIU over the SRI measurement ranging from 1 to 1.30, which, unlike the available LPFG sensors, may be applied to the humidity and vapor sensing. Meanwhile, the analysis method is applicable to the design of other types of birefringent-LPFG sensors.

Key words: Birefringence; Long-Period Fiber Grating (LPFG); Full-vector coupled mode theory; Stokes parameters; Optical fiber sensor

OCIS Codes: 060.3738; 060.2370;260.1440; 260.5430; 220.4610

0 Introduction

Long-Period Fiber Grating (LPFG) couples light from the core mode to cladding modes of a single-mode fiber, which can produce a series of attenuation bands at various resonant wavelengths in the transmission

Foundation item: The National Natural Science Foundation of China (No. 11004152), the National Basic Research Program of China (No. 2010CB327801)

First author: BAI Yu-kun (1970—), male, associate professor, Ph. D. degree, mainly focuses on fiber grating sensing technology. Email: tjutbai_1@163.com

Received: Jul. 2, 2015; **Accepted**: Aug. 25, 2015

spectrum[1]. The shift of resonant wavelength in response to certain external parameter forms the basis for the design of many types of optical LPFG sensors[2-4].

In practice, UV-induced LPFGs fabricated on low-intrinsic birefringence photosensitive optical fiber belong to the core-only photoinduced birefringence category[5]. Photoinduced birefringence can be attributed to one-sided exposure to UV light, which creates a larger Refractive Index (RI) change on the side of the core where the UV beam is impinged on[6], and the polarization of the writing beam[7]. Recently, T. A. Eftimov et al. experimentally demonstrated a SRI measurement method based on the LPFG polarization characteristics[8].

In this work, we performed a theoretical analysis of a SRI sensor based on the single-wavelength operation of a photoinduced core-only birefringent LPFG. To demonstrate the sensing principle, the LPFG with core-only photoinduced birefringence is analyzed using the full-vector coupled mode theory and the Stokes parameters, and the relationship between the defined polarization states' spherical distance on the Poincare sphere and the SRI n is established. Then, several practical design examples are enumerated, and the effects of the cladding-mode order and the cladding radius on the sensitivity are analyzed numerically. It is noteworthy that since the three-layer fiber model is more accurate than the two-layer counterpart for the core mode analysis[9-12], especially in the case of thin-cladding fiber, the effective RIs of the core mode and cladding modes are both calculated using the three-layer fiber model in the numerical analysis.

1 SRI sensing based on a LPFG with core-only photoinduced birefringence

For a uniform LPFG fabricated on a germanium-doped single-mode fiber through UV irradiation, the internal birefringence which includes the shape birefringence and stress birefringence can be neglected. However, in the presence of uneven UV-exposure in the LPFG fabrication process, different "dc" index changes[1] along the two principal axes of the optical fiber, namely the core-only photoinduced birefringence, should be taken into account. Generally, the photoinduced birefringence is on the order of 10^{-6}. The RI change of the fiber-core including the photoinduced birefringence can be written as

$$\Delta n_1^i(z)\approx(n_1\sigma(z)\pm\Delta n)(1+m\cos(2\pi z/\Lambda))\quad(i=x,\ y)\tag{1}$$

where "+" for $i=x$, and "−" for $i=y$, n_1 is the material RI of the fiber-core. $\sigma(z)$ is the slowly varying envelope of grating on the order of 10^{-4}. $n_1\sigma(z)$ is the "dc" index change without photoinduced birefringence. m is the fringe visibility of the index change. Λ is the grating period. Δn is the half "dc" index change difference induced by uneven UV-exposure between the two principal axes, i. e., the x and y axes, which, on the order of 10^{-6}, represents the photoinduced birefringence. The permittivity perturbation $\Delta\varepsilon^i(z)\approx 2\varepsilon_0 n_1\Delta n_1^i(z)$ is a function of z dependence, therefore, in the analysis of mode couplings, the coupling between LP_{01}^x and LP_{01}^y is neglected, and only the couplings between the core mode and cladding modes of the same polarization are taken into account.

In the presence of the fiber-core birefringence, the originally degenerated core modes LP_{01}^x and LP_{01}^y acquire a propagation constant difference $\Delta\beta=\beta_1^x-\beta_1^y$, which can be calculated from $\Delta\beta=\kappa_{co-co}^x-\kappa_{co-co}^y$[13], with κ_{co-co}^x and κ_{co-co}^y being the self-coupling coefficients of the core modes LP_{01}^x and LP_{01}^y, respectively. Since the "dc" index changes for both x and y polarizations are fairly small, the average propagation constant $\bar{\beta}=(\beta_1^x+\beta_1^y)/2$ is approximately equal to $\beta=2\pi n_{eff,co}/\lambda$, with $n_{eff,co}$ denoting the effective RI of the degenerated core modes. Therefore, the propagation constants for the x- and y-polarization core modes can be calculated from

$$\begin{aligned}\beta_1^x&=\beta+\Delta\beta/2\\ \beta_1^y&=\beta-\Delta\beta/2\end{aligned}\tag{2}$$

The full-vector coupled mode equations for LPFG[14] are

$$\begin{cases}\mathrm{d}A_1^i/\mathrm{d}z=\mathrm{j}A_1^i(z)\kappa_{co-co}^i\\ +\ \mathrm{j}A_2^i(z)\kappa^i\exp(-2\mathrm{j}\delta^i z)\\ \mathrm{d}A_2^i/\mathrm{d}z=\mathrm{j}A_1^i(z)\kappa^{i\,*}\exp(2\mathrm{j}\delta^i z)\\ +\mathrm{j}A_2^i(z)\kappa_{cl-cl}^i\end{cases}\quad(i=x,y)\tag{3}$$

where A_1^i and A_2^i are the electrical field amplitudes of the coupled core mode and cladding mode, respectively; $0\leqslant z\leqslant L$, L is the grating length; $\delta^i=0.5(\beta_1^i-\beta_2-2\pi/\Lambda)$ is the detuning factor, β_2 is the propagation constant of the coupled cladding mode, here the effective RIs or the propagation constants of the core mode and cladding modes are calculated using the three-layer fiber model[12]; κ_{co-co}^i is the self-coupling coefficient of the core mode, whereas κ_{cl-cl}^i is that of the cladding mode, which is small enough to be neglected, $\kappa^i=\kappa_{cl-co}^i/2$, κ_{cl-co}^i is the cross-coupling coefficient between the core mode and the cladding mode. In the cylindrical coordinate system (r,φ,z), the self-coupling coefficients of the core modes LP_{01}^x and LP_{01}^y are written as

$$\kappa_{co-co}^x(z)=0.5\omega\varepsilon_0 n_1(n_1\sigma(z)+\Delta n)\times\int_0^{2\pi}\mathrm{d}\varphi\int_0^{r_1}r\mathrm{d}r(|\boldsymbol{E}_r^{co}|^2\cos^2\varphi+|\boldsymbol{E}_\varphi^{co}|^2\sin^2\varphi)\tag{4}$$

$$\kappa^{y}_{co-co}(z) = 0.5\omega\varepsilon_0 n_1(n_1\sigma(z)-\Delta n)\times \int_0^{2\pi}\mathrm{d}\varphi\int_0^{r_1} r\mathrm{d}r(|\boldsymbol{E}^{co}_r|\sin^2\varphi+|\boldsymbol{E}^{co}_\varphi|\cos^2\varphi) \quad (5)$$

where ω is the angular frequency, and r_1 is the fiber-core radius. The cross-coupling coefficient between LP^x_{01} and the cladding mode is

$$\kappa^{x}_{cl-co}(z) = 0.5\omega\varepsilon_0 n_1(n_1\sigma(z)+\Delta n)\times \int_0^{2\pi}\mathrm{d}\varphi\int_0^{r_1} r\mathrm{d}r(\boldsymbol{E}^{cl}_r\boldsymbol{E}^{co\,*}_r\cos^2\varphi+\boldsymbol{E}^{cl}_\varphi\boldsymbol{E}^{co\,*}_\varphi\sin^2\varphi) \quad (6)$$

and that for LP^y_{01} is

$$\kappa^{y}_{cl-co}(z) = 0.5\omega\varepsilon_0 n_1(n_1\sigma(z)-\Delta n)\times \int_0^{2\pi}\mathrm{d}\varphi\int_0^{r_1} r\mathrm{d}r(E^{cl}_r\boldsymbol{E}^{co\,*}_r\sin^2\varphi+\boldsymbol{E}^{cl}_\varphi\boldsymbol{E}^{co\,*}_\varphi\cos^2\varphi) \quad (7)$$

With the input conditions $A^i_1(0)=1$ and $A^i_2(0)=0$, the core mode amplitudes derived from Eq. (3) are

$$A^i_1(z)=\left[\cos\left(\sqrt{\kappa^i\kappa^{i\,*}+(\bar{\sigma}^i)^2}\,z\right)+\mathrm{j}\bar{\sigma}^i\left(1/\sqrt{\kappa^i\kappa^{i\,*}+(\bar{\sigma}^i)^2}\right)\times\sin\left(\sqrt{\kappa^i\kappa^{i\,*}+(\bar{\sigma}^i)^2}\,z\right)\right]\times \exp(\mathrm{j}\kappa^i_{co-co}z/2)\exp(-\mathrm{j}\delta^i z) \quad (i=x,\ y) \quad (8)$$

The electric fields of the core modes LP^x_{01} and LP^y_{01} along a LPFG can be written as

$$\begin{cases} E_x = A^x_1(z)\exp(-\mathrm{j}\beta^x_1 z+\mathrm{j}\delta_x) \\ E_y = A^y_1(z)\exp(-\mathrm{j}\beta^y_1 z+\mathrm{j}\delta_y) \end{cases} \quad (9)$$

with the initial phases δ_x, δ_y being constant.

Assuming that the incident light is a completely-polarized light, its Stokes parameters are given by[15]

$$\begin{cases} s_0 = E_xE_x^* + E_yE_y^* \\ s_1 = E_xE_x^* - E_yE_y^* \\ s_2 = E_x^*E_y + E_xE_y^* \\ s_3 = -\mathrm{j}(E_x^*E_y - E_xE_y^*) \end{cases} \quad (10)$$

which can be normalized against s_0 by letting $s_0=1$. These parameters s_i $(i=1,2,3)$ are three-dimensional coordinates, and can be described by a point on the surface of the Poincare sphere. To calculate the spherical distance, the three-dimensional coordinates s_i $(i=1,2,3)$ are converted into latitude and longitude coordinates as follows

$$\begin{cases} 2\chi = \arctan\left(s_3/\sqrt{s_1^2+s_2^2}\right) \\ 2\varphi = \begin{cases} \arctan(s_2/s_1), & s_1>0 \\ \pi+\arctan(s_2/s_1), & s_1<0, s_2>0 \\ \arctan(s_2/s_1)-\pi, & s_1<0, s_2<0 \end{cases} \end{cases} \quad (11)$$

where 2χ is latitude (Unit: radian), 2φ is longitude (Unit: radian), and the radius of the Poincare sphere is $r=1$ (dimensionless).

With the assumption that on the Poincare sphere the latitude and longitude of point A are $2\chi_1$ and $2\varphi_1$, respectively, and that of point B are $2\chi_2$ and $2\varphi_2$, the spherical distance, namely the minor arc length, between points A and B is

$$l_{AB} = r\cdot\arccos(\sin(2\chi_1)\sin(2\chi_2)+\cos(2\chi_1)\cdot\cos(2\chi_2)\cos(2\varphi_1-2\varphi_2)) \quad (12)$$

For the incident completely-polarized light with a given wavelength of λ, the LPFG output polarization state for SRI $n=1$ is denoted as point p_0 on the Poincare sphere. When the SRI varies from 1 to some other value n (no more than the cladding material RI), the corresponding output polarization state on the Poincare sphere varies from p_0 to another point p. The spherical distance l between points p_0 and p can be calculated from Eq. (12). Therefore we can use the spherical distance l with the reference point fixed at p_0 to represent the SRI n. Furthermore, the measurement sensitivity can be defined as

$$\mathrm{Slope\_arc} = \mathrm{d}l/\mathrm{d}n \quad (13)$$

which is dimensionless.

2 Numerical analysis

In this section, practical design examples of the birefringent-LPFG SRI sensors are provided and the sensing characteristics for the cladding radii of 62.5 μm, 31.5 μm and 20.75 μm are analyzed numerically. The incident light is a completely-polarized light, whose wavelength approximates the resonant wavelength for the mode coupling between the core mode and a specific cladding mode in the air. The couplings to the first-order and third-order cladding modes (with the azimuthal order $\mu=1$) are of our concern. The parameters of LPFG are specified as follows: fiber-core radius 4.15 μm, grating length 1.5 cm, grating period 320μm; fiber-core material RI 1.4681, cladding material RI 1.4628; the slowly varying envelope of grating $\sigma=2.25\times10^{-4}$ and the core-only photoinduced birefringence $\Delta n=5\times10^{-6}$.

When the SRI varies from 1 to 1.46 with a step of 0.01, the corresponding output polarization state evolution on the Poincare sphere for the cladding radii of 62.5 μm, 31.5 μm and 20.75 μm is illustrated in Fig. 1. In the process, it is assumed that a completely-polarized light with a single wavelength equal to the resonant wavelength for the x-components of the core mode and the first-order cladding mode or the third-order cladding mode (with the azimuthal order $\mu=1$) is launched into the LPFG. The incident wavelength should be close to the specific resonant wavelength to achieve the desired mode coupling and a larger sensitivity. The R dot and G dot on the Poincare sphere

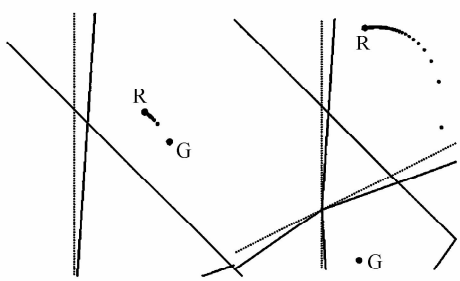

(a) The first-order at Rcladding= 62.5μm and λ=795nm (b) The first-order at Rcladding= 31.5μm and λ=862nm

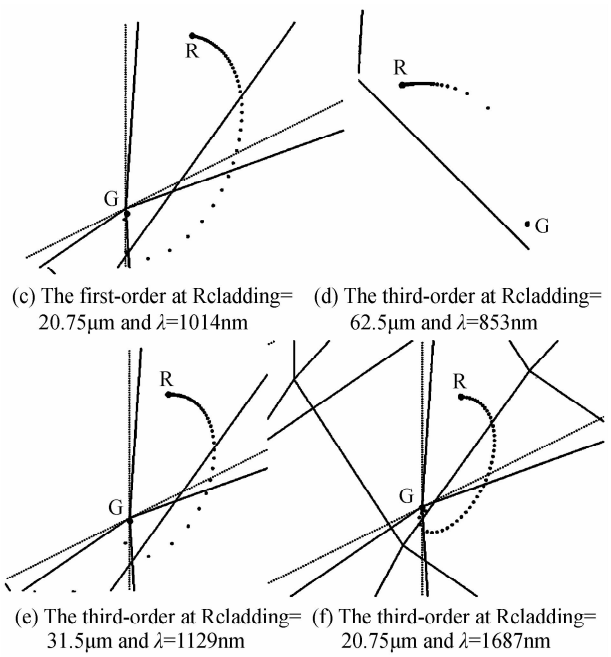

Fig. 1 Output light polarization evolution on the Poincare sphere for different couplings

represent the polarization states of the output light for SRI $n=1$ and 1.46, respectively.

According to the defined spherical distance l corresponding to a SRI, we can derive the relationship between l and SRI n for the given SRI series, as shown in Fig. 2. For the LPFG with a cladding radius of 20.75 μm, the relationship between the spherical distance and SRI over a measurement range from 1 to 1.30 is approximately linear, which makes it ideal for the humidity and vapor sensing. The sensitivity is approximately 0.07754/RIU for the first-order cladding mode and 0.356/RIU for the third-order cladding mode in addition to the fact that the sensor coupling to the third-order cladding mode has better linearity performance than that coupling to the first-order cladding mode in the specified SRI measurement range.

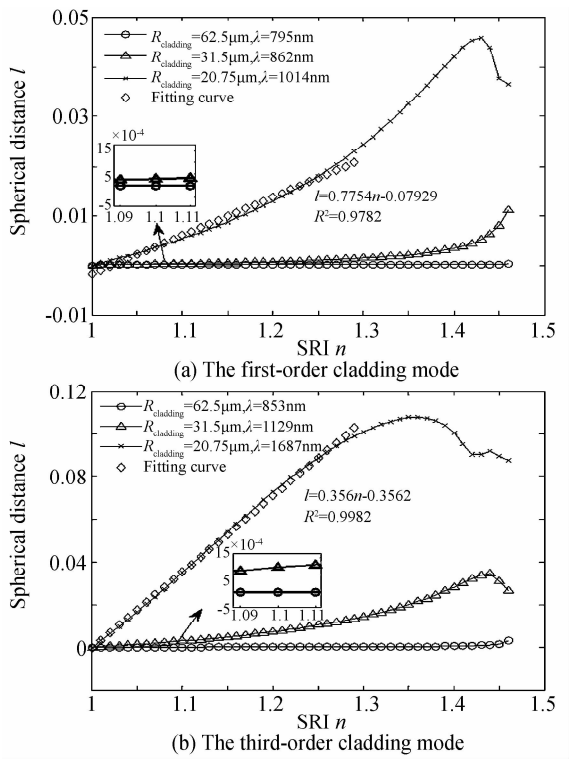

Fig. 2 Spherical distance l versus SRI n with various cladding radii for the couplings

The corresponding sensitivity over the measurement range from 1 to 1.46 is shown in Fig. 3. As seen in the figure, within the SRI measurement range from 1 to 1.30 the LPFG with a cladding radius of 20.75 μm shows the maximum sensitivity, whereas with a cladding radius of 62.5 μm the sensitivity is the minimum. Moreover, the sensitivity for the third-order cladding mode is larger than that for the first-order cladding mode. Compared with the conventional LPFG sensors[16-18] and the LPFG sensors introduced in Ref. [8], which make SRI measurement in the range of 1.32 to 1.46 with a small range of linear sensitivity, our SRI sensor demonstrates a broad linear measurement range from 1 to 1.30.

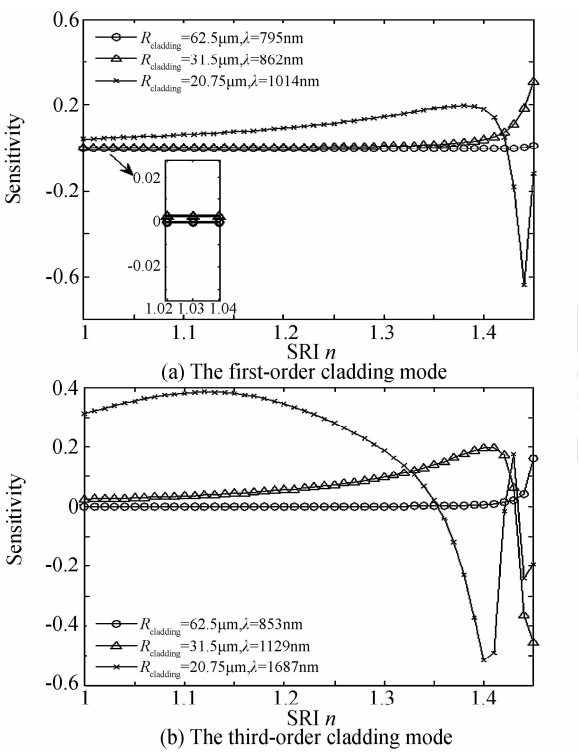

Fig. 3 Sensitivity versus SRI n with various cladding radii for the couplings

It is worthwhile to note that the analysis method based on the full-vector coupled mode theory and Stokes parameters can be applied to the design of torsion- or shape-induced-birefringence LPFG sensors for SRI or temperature measurements by appropriately modeling the birefringence.

3 Conclusion

Based on the core-only photoinduced birefringence of LPFG, we propose and theoretically demonstrate a method for the SRI sensing. The incident light is a completely-polarized light with the wavelength approximating a particular resonant wavelength of the LPFG in the air. The defined spherical distance l versus SRI n on the Poincare sphere with various cladding radii for the couplings to the first-order cladding mode and the third-order cladding mode are investigated. The result indicates that the LPFG-based sensor with a cladding radius of 20.75 μm shows a good linearity performance and high sensitivity over the SRI measurement range from 1 to 1.30, which may be applied to the humidity and vapor sensing. The birefringent-LPFG sensing scheme and its analysis method based on the full-vector coupled mode theory can be readily applied to the design of other types of LPFG-based sensors.

Reference

[1] WANG Y P. Review of long period fiber gratings written by CO_2 laser[J]. *Journal of Applied Physics*, 2010, **108**(8): 081101.

[2] DENG C L, GU Z T, ZHANG J T. Resonant characteristics and optimization of long period fiber grating coated with weak absorption double-layer films [J]. *Acta Photonica Sinica*, 2009, **38**(11): 2873-2879.

[3] JIN Q L, HUANG X H, YAN L F, *et al*. Optimization of long-period fiber grating for refractive-index sensor[J]. *Acta Photonica Sinica*, 2011, **40**(8): 1201-1204.

[4] SHI L L, ZHU T, FAN Y E, *et al*. Torsion sensing with a fiber ring laser incorporating a pair of rotary long-period fiber gratings[J]. *Optics Communications*, 2011, **284**(22): 5299-5302.

[5] BRENT L B, THOMAS K G. Polarization-dependent loss and birefringence in long-period fiber gratings[J]. *Applied Optics*, 2004, **42**(34): 6816-6823.

[6] SU Y, ZHANG B F, ZHU Y, *et al*. Sensing circular birefringence by polarization-dependent parameters in fiber Bragg gratings and the influence of linear birefringence[J]. *Optical Fiber Technology*, 2012, **18**(1): 51 - 57.

[7] PHILIP O, PAWEL N. Polarization-switching FBG interrogator for distributed point measurement of magnetic field strength and temperature[J]. *Sensors Journal IEEE*, 2011, **11**(5): 1220-1226.

[8] TINKO E, WOJTEK B, PREDRAG M, *et al*. Single-wavelength polarization-sensitive interrogation of a long-period grating (LPG) sensor [J]. *Measurement Science and Technology*, 2010, **21**: 1299-1304.

[9] TURAN E. Cladding-mode resonances in short- and long-period fiber grating filters[J]. *Journal of the Optical Society of America A*, 1997, **14**(8): 1760-1773.

[10] TURAN E. Cladding-mode resonances in short-and long-period fiber grating filters: errata[J]. *Journal of the Optical Society of America A*, 2000, **17**(11): 2113.

[11] CHARLES T. Optical Fibre Waveguide Analysis[M], UK: Oxford Science Publications, 1992.

[12] CAO H X, BAI Y K, LI J H, *et al*. Analysis of sensing characteristics of a long-period fiber grating based on two fiber analysis models[J]. *Chinese Journal of Laser*, 2014, **41**(2): 250-258.

[13] NOBUYUKI I, NOBUYUKI Y, JUN I S, *et al*. Birefringence in single-mode optical fiber due to elliptical core deformation and stress anisotropy [J]. *IEEE Journal of Quantum Electronics*, 1980, QE-**16**(11): 1267 - 1271.

[14] LU Y C, HUANG W P, JIAN S S. Full vector complex coupled mode theory for tilted fiber gratings [J]. *Optics Express*, 2010, **18**(2): 713-26.

[15] GIORGIO F, CYNTHIA P S. Representation of the polarization of single-mode fibers using Stokes parameters [J]. *Journal of the Optical Society of America*, 1981, **71**(12): 1487-1491.

[16] FAN Y, ZHU T, SHI L, *et al*. Highly sensitive refractive index sensor based on two cascaded special long-period fiber gratings with rotary refractive index modulation[J]. *Applied Optics*, 2011, **50**(23): 4604-4610.

[17] GUAN C Y, TIAN X Z, LI S Q, *et al*. Long period fiber grating and high sensitivity refractive index sensor based on hollow eccentric optical fiber [J]. *Sensors & Actuators B Chemical*, 2013, **188**(11): 768-771.

[18] QI L, ZHAO C L, YUAN J Y, *et al*. Highly reflective long period fiber grating sensor and its application in refractive index sensing[J]. *Sensors & Actuators B Chemical*, 2014, **193**(3): 185 - 189.